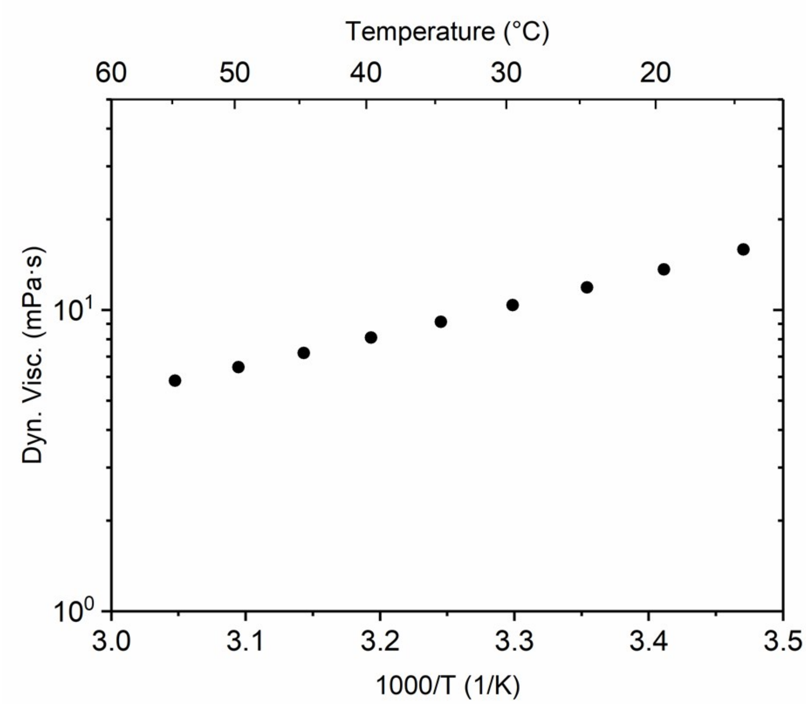

Fig. S1. Arrhenius plot of dynamic viscosity for 2.5 m LiFSI and 0.2 m LiPF6 in the FSA solvent

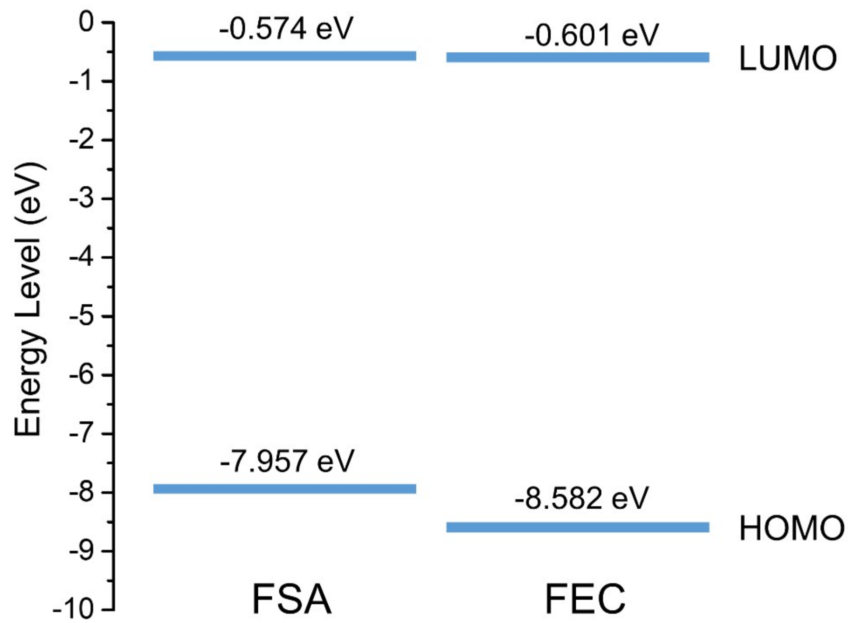

Fig. S2 The lowest unoccupied molecular orbital (LUMO) and the highest occupied molecular orbital (HOMO) energy values of FSA and FEC obtained by DFT simulations

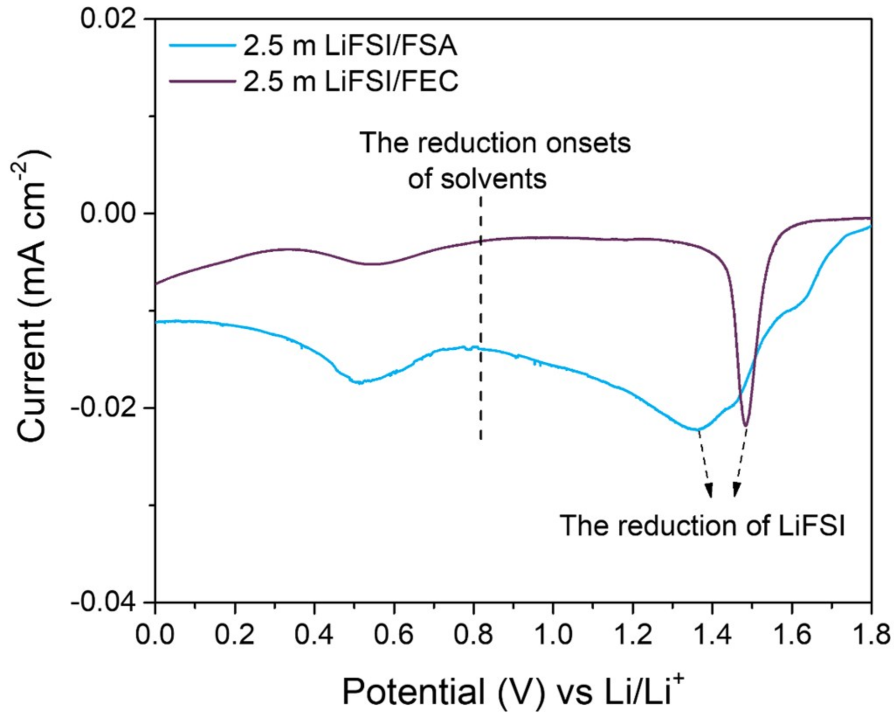

Fig. S3 Linear sweep voltammetry (LSV) results of the electrolytes with 2.5 m LiFSI in FEC or FSA at a scan rate of 0.2 mV s^{-1} tested in coin cells with Li and Cu as the working and counter electrodes, respectively.

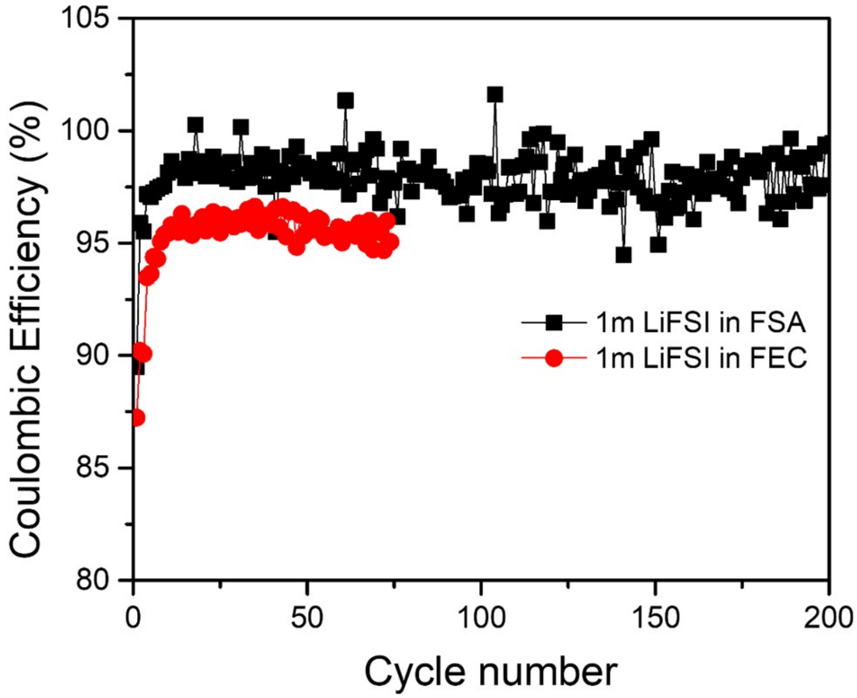

Fig. S4 Li stripping/plating CEs using 1 m LiFSI in FSA and 1 m LiFSI in FEC electrolytes. The current density is 0.5 mA cm^{-2} and capacity 0.5 mAh cm^{-2}.

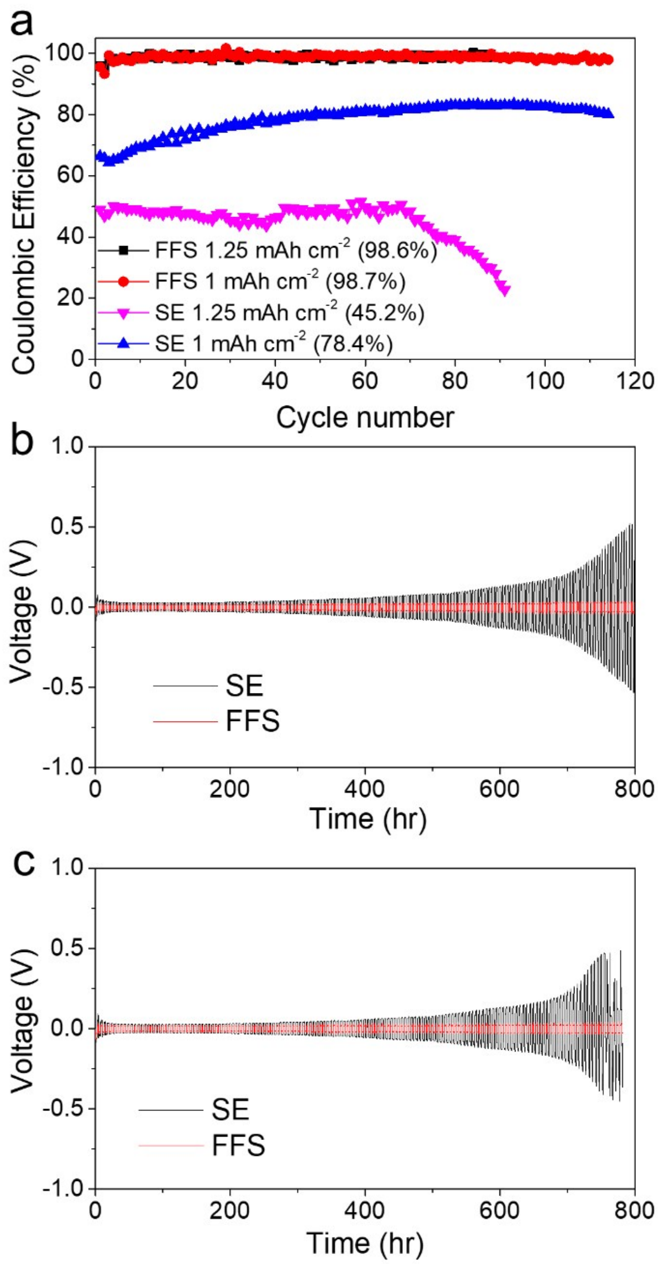

Fig. S5 Electrochemical performances of the Li plating/stripping in FFS and SE electrolytes. (a) Li plating/stripping CEs evaluated by Li||Cu coin cells (1 and 1.25 mAh cm^{-2} at 0.5 mA cm^{-2}); Li||Li plating/stripping from Li||Li symmetric cells with 1 mAh cm^{-2} (b) and 1.25 mAh cm^{-2} (c) at 0.5 mA cm^{-2}, respectively.

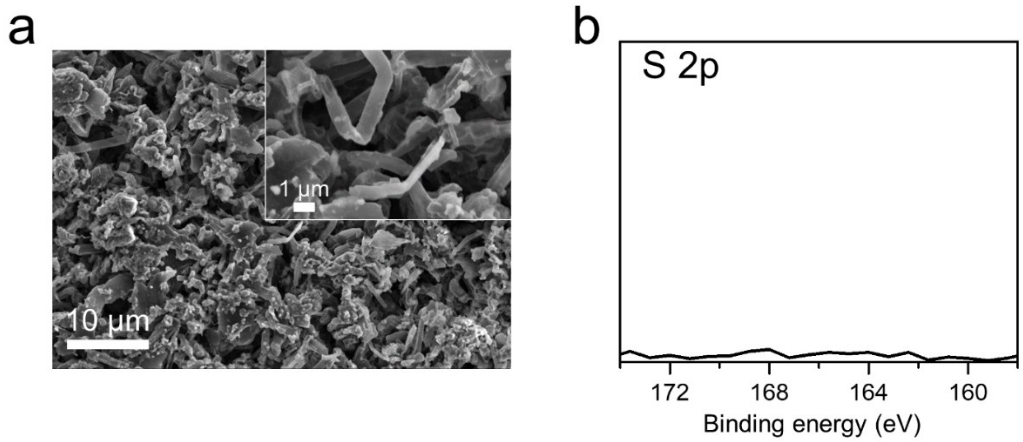

Fig. S6 Characterization of the cycled Li in SE (10 cycles, 0.5 mA cm^{-2}, 0.5 mAh cm^{-2}). (a) SEM figure (inset is the high resolution figure); (b) S 2p spectrum from XPS analysis.

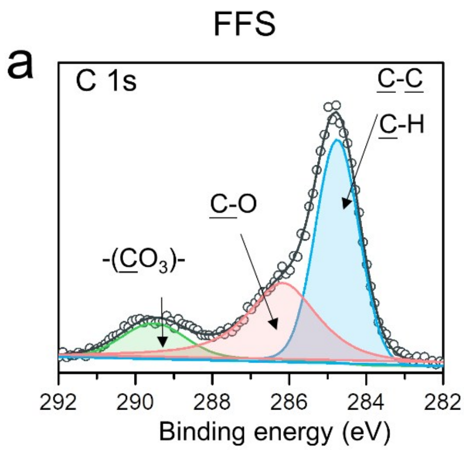

Fig. S7 XPS spectra (C 1s) of the cycled Li in FFS (a) and LFF (b) electrolytes (10 cycles, 0.5 mA cm^{-2}, 0.5 mAh cm^{-2})

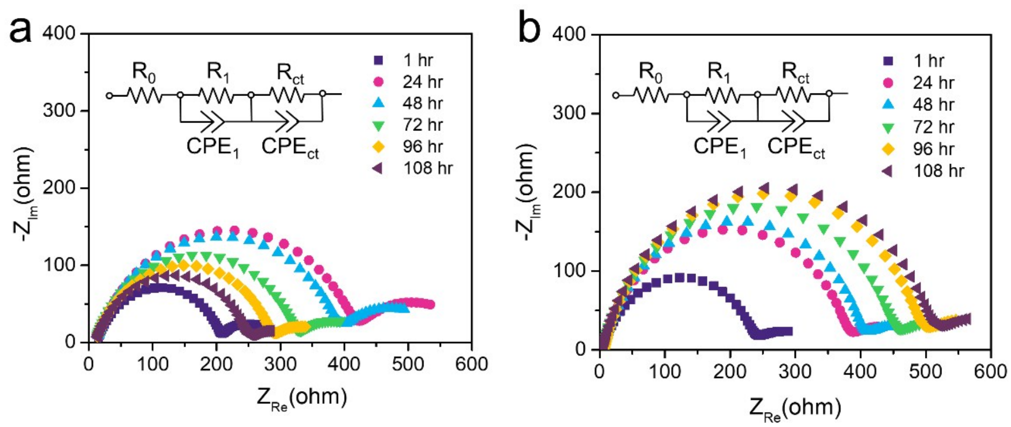

Fig. S8 The evolution of impedance spectra of the Li||Li symmetric cell with resting time in LFF (a) and SE (b) electrolytes.

The wettability of FEC-based LFF electrolyte is so poor that glass fiber separator with large pores and hydrophilic surface has to be used instead of the Celgard separator to improve wetting. Therefore, for LFF electrolyte, the time-consuming wetting process should also contribute to R_1 (R_1=R_{SEI}+$R_{wetting}$). When the wetting proceeds upon resting time, $R_{wetting}$ decreases quickly resulting in the decrease in R_1.

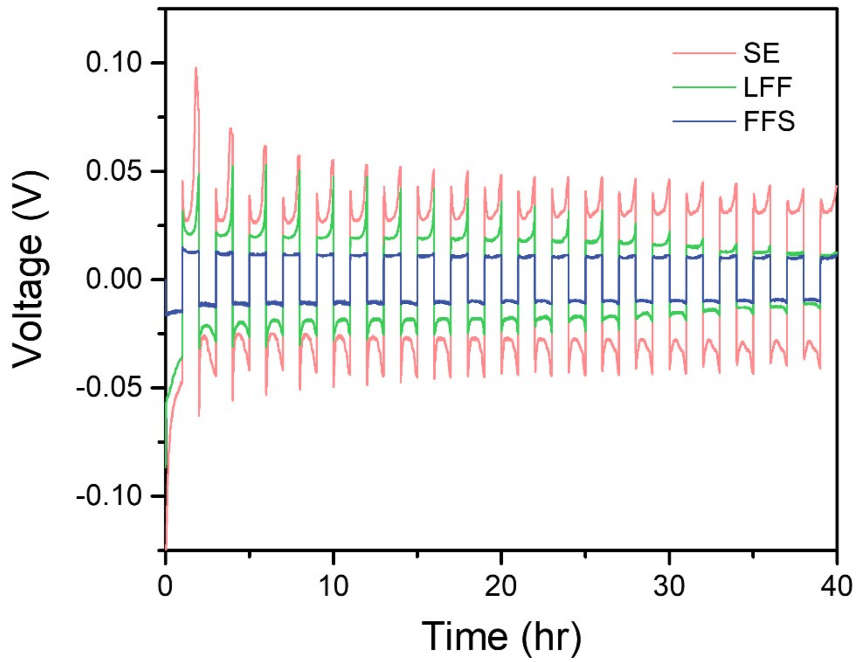

Fig. S9 The initial cycles of the Li||Li symmetric cells in different electrolytes tested after 108 hr rest. All cells were operated at a current density of 0.5 mA cm^{-2} with a capacity of 0.5 mAh cm^{-2}

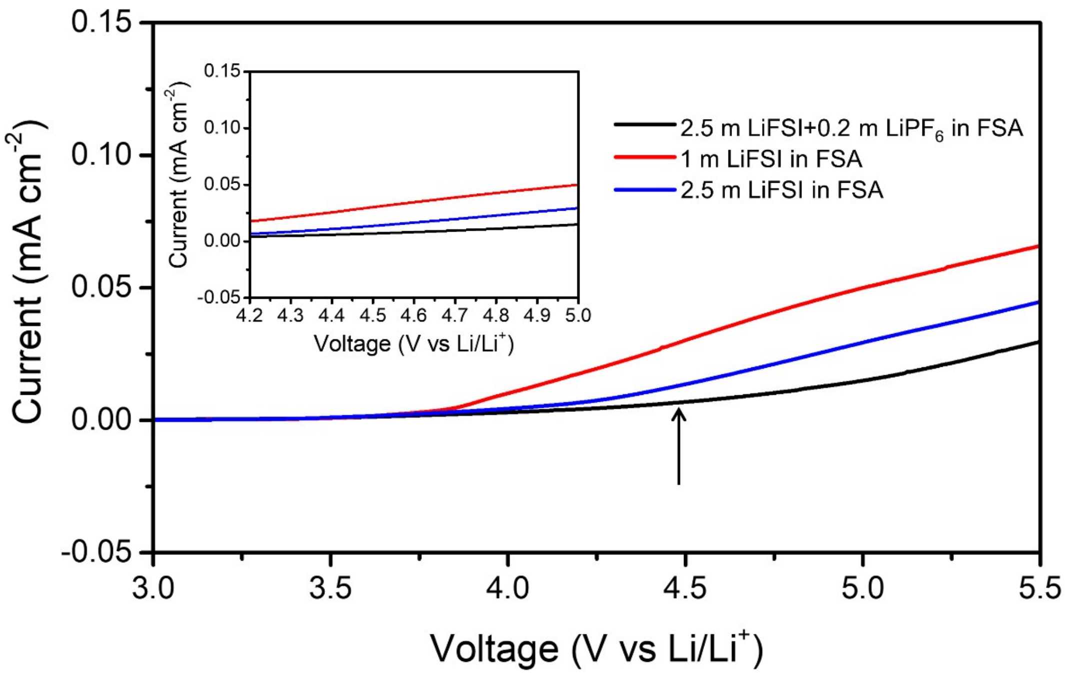

Fig. S10 LSV results of the anodic stability of Al electrodes by using Li||Al coin cells within 3.0 V~5.5 V using 1 m LiFSI in FSA, 2.5 m LiFSI in FSA and 2.5 m LiFSI+0.2 m $LiPF_6$ in FSA electrolytes. The addition of 0.2 m $LiPF_6$ obviously suppresses the Al corrosion for 2.5 m LiFSI in FSA electrolyte improving the anodic stability to ~ 4.5 V which fulfills the requirement for the NMC622 cathode. Inset: magnified view of 4.2~5.0 V region.

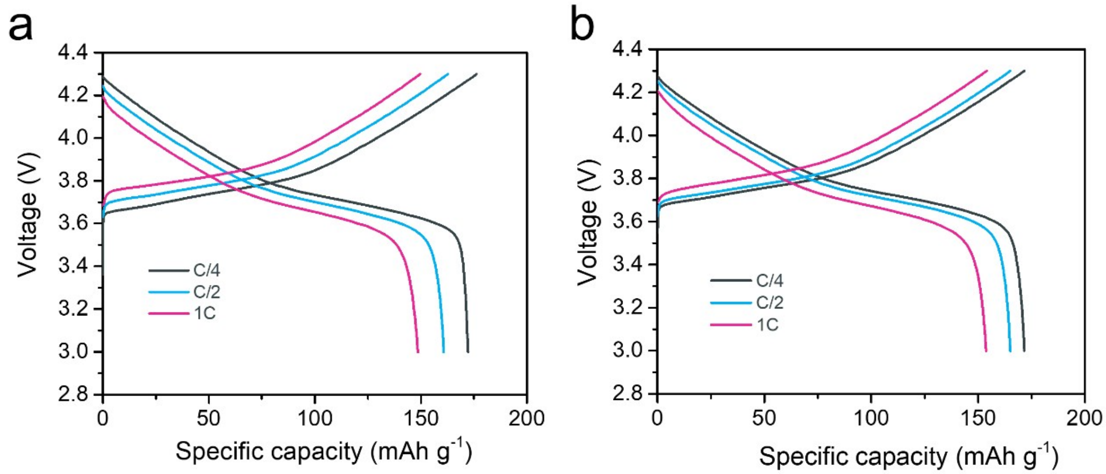

Fig. S11 Voltage profiles of the Li||NMC622 cells using the SE (a) and LFF (b) electrolytes at C/4, C/2 and 1C

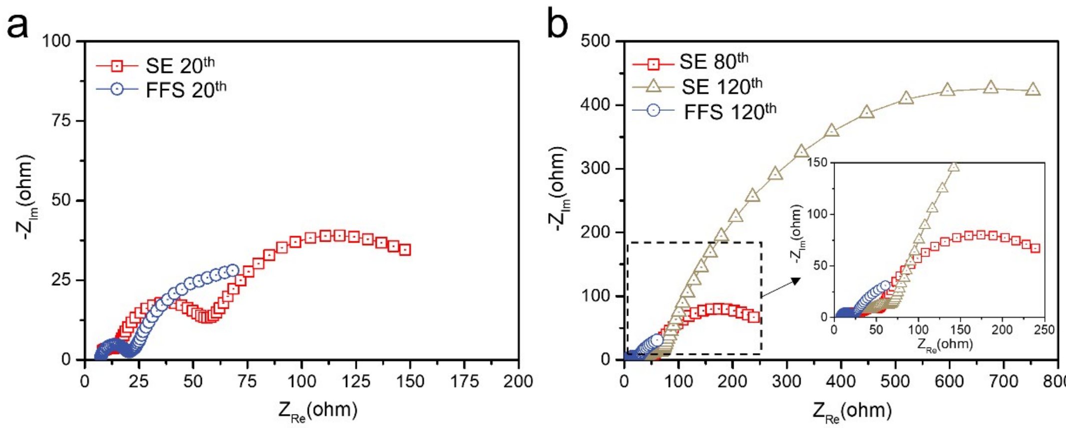

Fig. S12 The evolution of impedance spectra of the Li||NMC622 cells in FFS and SE electrolytes after 20th (a) and 80th/120th (b) cycles

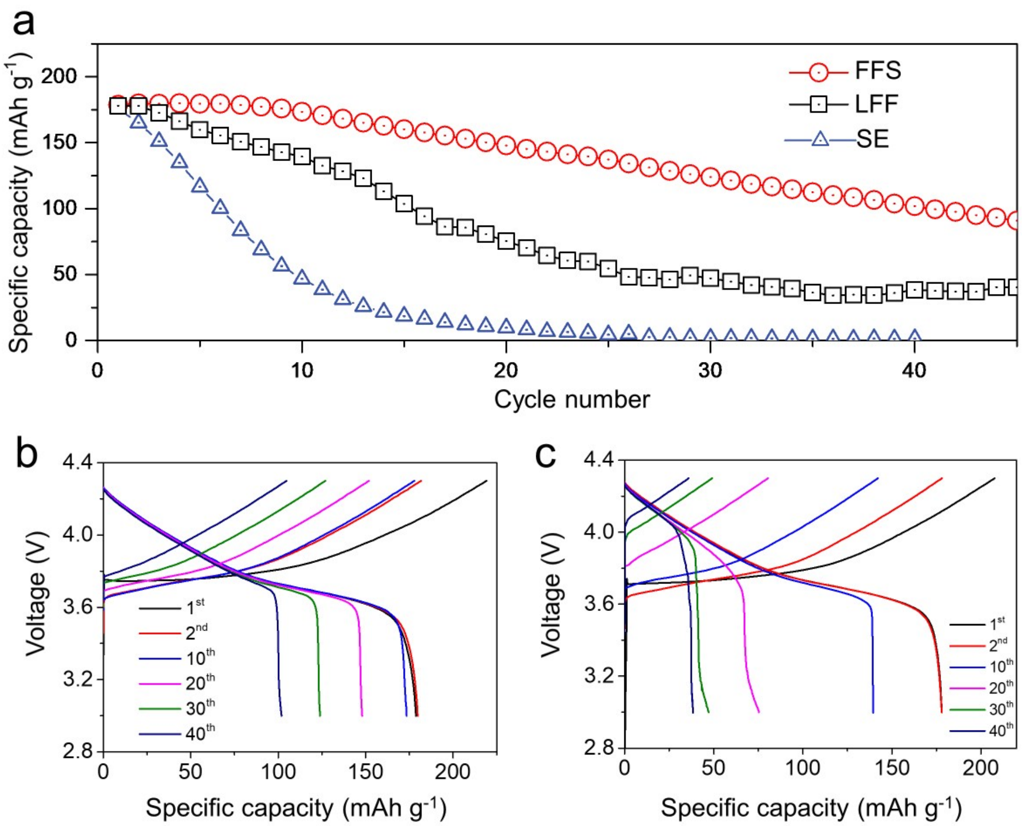

Fig. S13 The electrochemical performances of the anode-free full cells (Cu||NMC622) using FFS, LFF and SE electrolytes. (a) Cycling performance. The charge-discharge voltage profiles (1^{st}, 2^{nd}, 10^{th}, 20^{th}, 30^{th} and 40^{th} cycle) of the cells using FFS (b) and LFF (c) electrolytes.

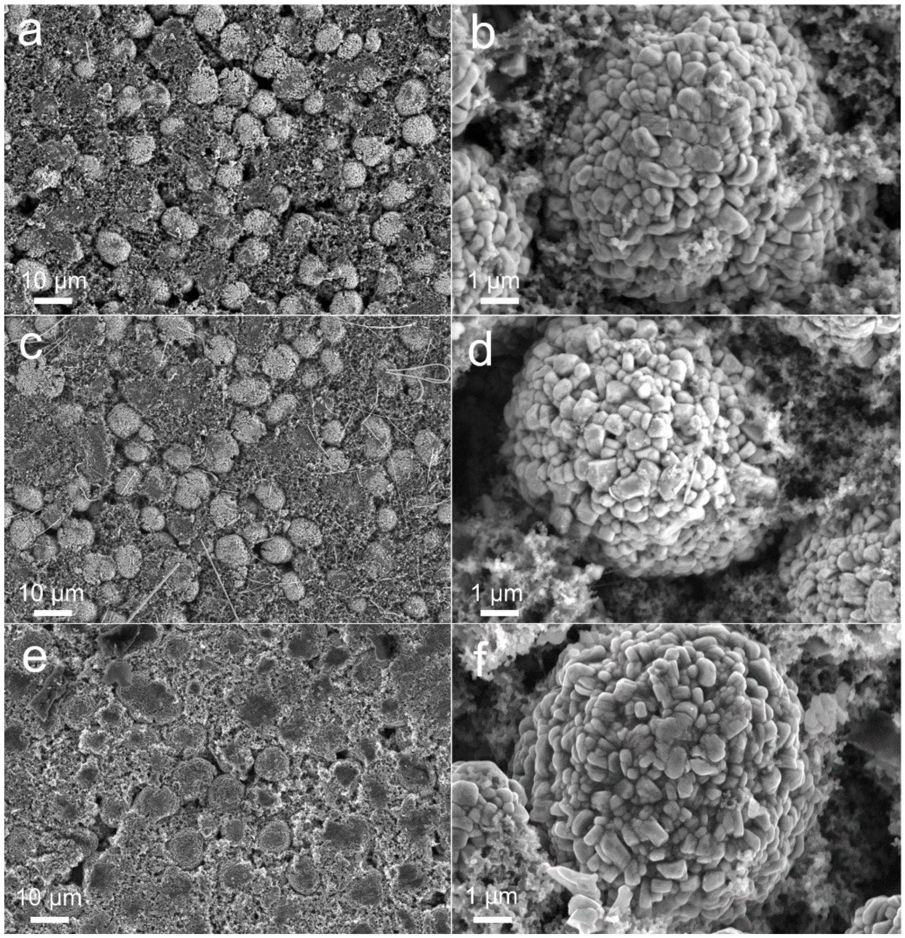

Fig. S14 SEM figures with low and high magnification of the NMC622 cathodes after 100 cycles at 0.5 C in FFS (a, b), LFF (c, d) and SE (e, f) electrolytes

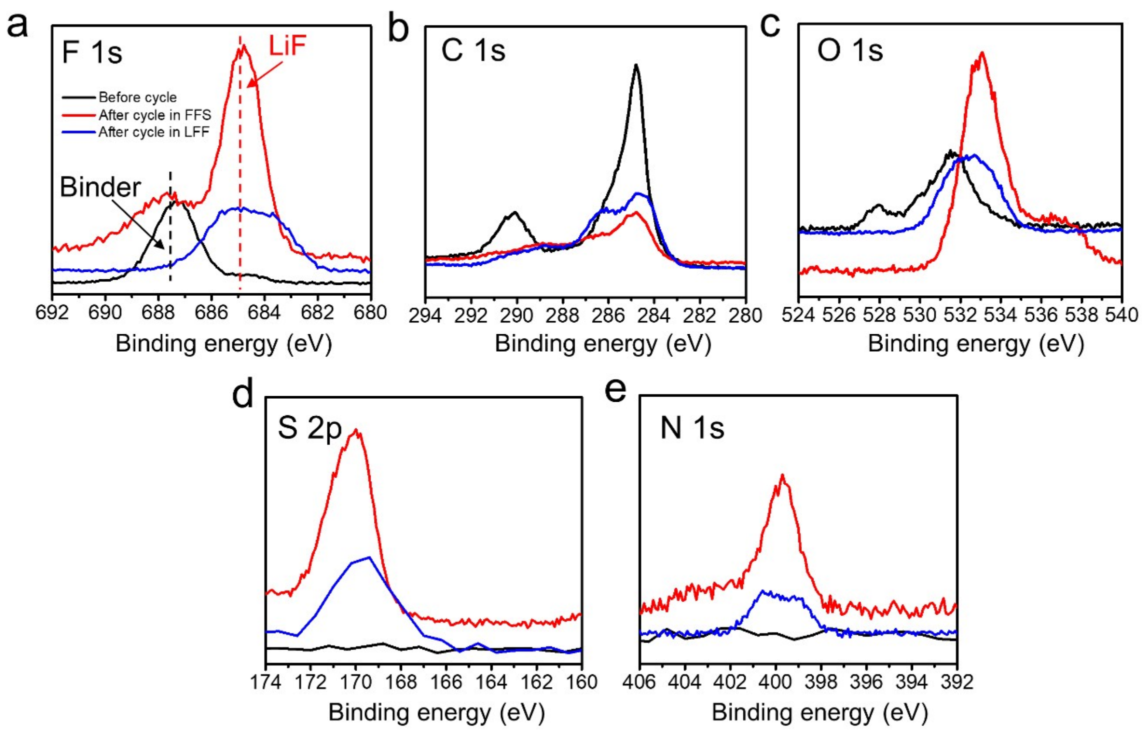

Fig. S15 XPS spectra of the NMC622 cathodes before (black line) and after 100 cycles at 0.5 C in FFS (red line) and LFF (blue line) electrolytes. (a) F 1s, (b) C 1s, (c) O1s, (d) S 2p, (e) N 1s.

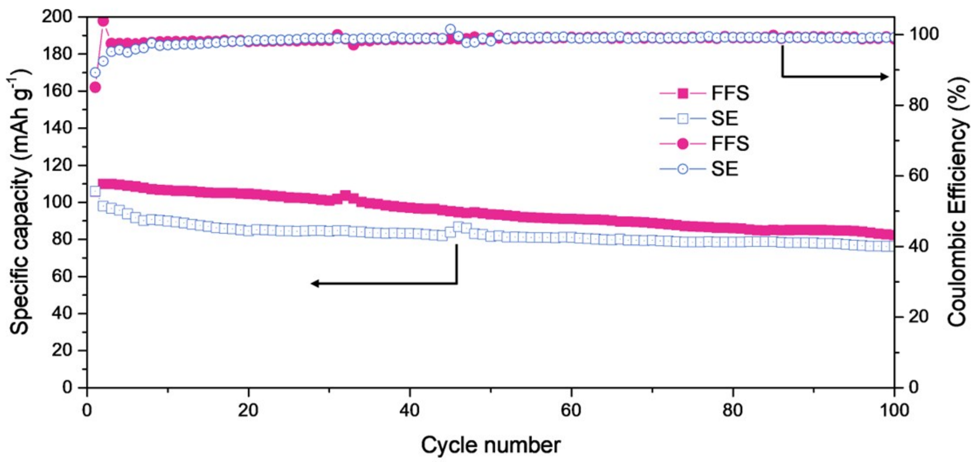

Fig. S16 Cycling performance of the Li||$LiMn_2O_4$ cells with FFS and SE electrolytes. The cells were cycled at 0.5 C from 3.0 V to 4.3 V.

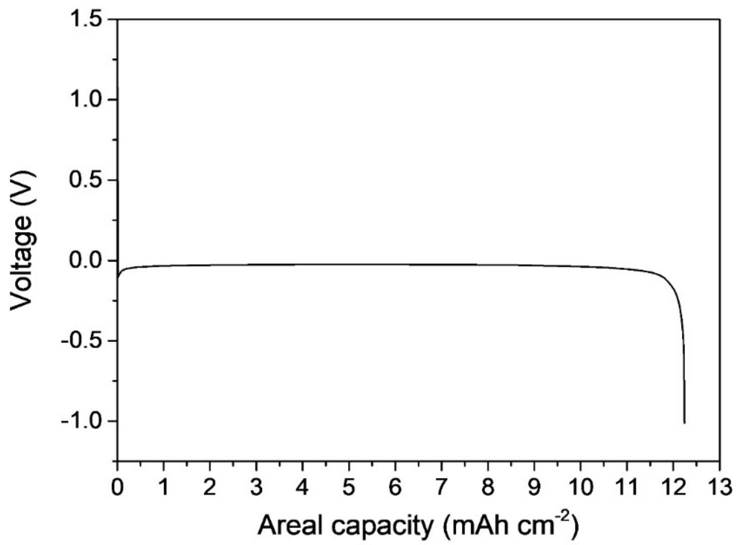

Fig. S17 The areal capacity of the thin Li (60 μm) foil evaluated by a Li||Cu cell

Table S1. Dynamic viscosity and density as a function of temperature for 2.5 m LiFSI and 0.2 m $LiPF_6$ in the FSA solvent.

Temperature (°C)	Dyn. Visc. (mPa·s)	Shear Rate (s^{-1})	Density (g cm^{-3})
15	15.880	432.9	1.49667
20	13.640	467.5	1.49024
25	11.875	498.9	1.48388
30	10.378	529.7	1.47738
35	9.1283	558.0	1.47121
40	8.0982	585.0	1.46501
45	7.2001	611.3	1.45898
50	6.4557	634.7	1.45274
55	5.8270	655.2	1.44660

Table S2. Comparison of our work with recent excellent works on electrolytes for LMBs

Category	Composition	Lithium metal side (evaluated by Li-Cu cells)				Cathode side (>4.0 V)	High concentration	Pretreatment of substrate†
		Current density	Initial CE (ICE)	ECN*	Average CE			
New electrolyte	**2.5 m LiFSI+0.2 m $LiPF_6$ in FSA**	**0.5 mA cm^{-2}**	**91%**	**10**	**99.03%**	**YES**	**NO**	**NO**
Carbonate-based	10 M LiFSI in DMC[1]	0.2 mA cm^{-2}	~89%	>80	~98.7%#	YES	YES	NO
	7 m LiFSI in FEC[2]	0.5 mA cm^{-2}	~89%#	>300#	~97.72%	YES	YES	NO
	1 M $LiPF_6$ in FEC/FEMC/HFE[3]	0.5 mA cm^{-2}	~92%	>100#	< 99%	YES	NO	NO
Sulfone-based	LiFSI-3TMS-3TTE[4]	0.5 mA cm^{-2}	—	~20#	98.8%	YES	NO	5 mAh cm^{-2} Li pre-deposited and stripped
Ether-based	LiTFSI+$LiNO_3$+LiFSI in DME[5]	0.5 mA cm^{-2}	92%	—	99.1%	NO	NO	NO
	4 M LiFSI in DME[6]	0.2 mA cm^{-2}	—	—	99.1%	NO	YES	NO
	4.6 m LiFSI+ 2.3 m LiTFSI in DME[7]	0.5 mA cm^{-2}	82.11%	—	97.9%	YES	YES	NO
	1.2 m LiFSI in DMC-BTFE[8]	0.5 mA cm^{-2}	~93%#	~30#	~99%	YES	NO	NO
	2 M LiTFSI + 2 M LiDFOB in DME[9]	—	—	—	94.6%	YES	YES	NO
	LiFSI-1.2DME-3TTE[10]	0.5 mA cm^{-2}	—	13#	>99.3%	YES	NO	NO

†Substrates after pretreatments may possibly result in improved CE values compared to those without pretreatment

*Essential cycle number (ECN) from ICE to >99%

#Estimated values, could not find the exact numbers in texts

Supplementary List List of abbreviations (arranged in alphabetical order)

CE: Coulombic Efficiency

CEI: Cathode Electrolyte Interface

CI: Coulombic Inefficiency

DFT: Density Functional Theory

DEC: Diethyl Carbonate

DMC: Dimethyl Carbonate

DOL: Dimethoxyethane

EC: Ethylene Carbonate

ECN: Essential Cycle Number from ICE to SCE

EIS: Electrochemical Impedance Spectroscopy

FEC: Fluoroethylene Carbonate

FFS: Full Fluorosulfonyl (electrolyte)

FSA: Fluorosulfonamide

HCEs: High Concentration Electrolytes

HOMO: Highest Occupied Molecular Orbital

ICE: Initial Coulombic Efficiency

LFF: LiFSI in FEC (electrolyte)

LIBs: Lithium-ion Batteries

LiFSI: Lithium Bis(fluorosulfonyl)imide

LHCEs: Localized High Concentration Electrolytes

LMA: Lithium Metal Anode

LMBs: Lithium Metal Batteries

LSV: Linear Sweep Voltammetry

LUMO: Lowest Unoccupied Molecular Orbital

NMC622: $LiNi_{0.6}Mn_{0.2}Co_{0.2}O_2$

SCE: Stabilized Coulombic Efficiency

SE: Standards Electrolyte

SEI: Solid Electrolyte Interface

SEM: Scanning Electron Microscope

XPS: X-ray Photoelectron Spectroscopy

XRD: X-ray Diffraction

Supplementary References

1. Fan X*, et al.* Highly Fluorinated Interphases Enable High-Voltage Li-Metal Batteries. *Chem* **4**, 174-185 (2018).

2. Suo L*, et al.* Fluorine-donating electrolytes enable highly reversible 5-V-class Li metal batteries. *Proceedings of the National Academy of Sciences of the United States of America* **115**, 1156-1161 (2018).

3. Fan X*, et al.* Non-flammable electrolyte enables Li-metal batteries with aggressive cathode chemistries. *Nature nanotechnology*, (2018).

4. Ren X*, et al.* Localized High-Concentration Sulfone Electrolytes for High-Efficiency Lithium-Metal Batteries. *Chem* **4**, 1877-1892 (2018).

5. Feilong Qiu*, et al.* A Concentrated Ternary-Salts Electrolyte for High ReversibleLi Metal Battery with Slight Excess Li. *Adv Energy Mater*, 1803372 (2018).

6. Qian J*, et al.* High rate and stable cycling of lithium metal anode. *Nat Commun* **6**, 6362 (2015).

7. Alvarado J*, et al.* Bisalt ether electrolytes: a pathway towards lithium metal batteries with Ni-rich cathodes. *Energy & Environmental Science* **12**, 780-794 (2019).

8. Chen S*, et al.* High-Voltage Lithium-Metal Batteries Enabled by Localized High-Concentration Electrolytes. *Adv Mater*, e1706102 (2018).

9. Jiao S*, et al.* Stable cycling of high-voltage lithium metal batteries in ether electrolytes. *Nat Energy* **3**, 739-746 (2018).

10. Ren X*, et al.* Enabling High-Voltage Lithium-Metal Batteries under Practical Conditions. *Joule*, (2019).